



# Can kurtosis be an early warning signal for abrupt climate change?

Xiao-qiang Xie<sup>1,2,3</sup> · Wen-ping He<sup>2,3</sup>  · Bin Gu<sup>1,2</sup> · Ying Mei<sup>1,2,3</sup> · Shan-shan Zhao<sup>2,3</sup>

Received: 3 July 2018 / Accepted: 21 November 2018 / Published online: 28 November 2018  
© Springer-Verlag GmbH Germany, part of Springer Nature 2018

## Abstract

The climate system occasionally experiences an abrupt change. However, it is very difficult to predict this change at present. Fortunately, some generic properties have been revealed before several different types of dynamical system near their own critical thresholds. These properties provide a possible way to give an early warning for an impending abrupt climate change. Therefore, it is important to evaluate the applicability of an early warning indicator of an abrupt change. On the basis of several simple fold models, we have systematically investigated the performance of the kurtosis coefficient as an early warning signal for an upcoming abrupt climate change. The testing results indicate that the kurtosis coefficient is a reliable warning indicator in most of cases whether a critical control parameter or the strength of an external forcing approaches a critical point. However, the strong noise can greatly shorten the effective warning time, and also can result in the reduction of the magnitude of a kurtosis coefficient when a dynamical system approaches its critical threshold. The missing data has almost no effect on the kurtosis coefficient in all of tests, even it is true when the missing data accounts for 20% of the total sample. We also found that the kurtosis coefficient does not work in some cases, which means that the kurtosis coefficient is not a universal early warning signal for an upcoming abrupt change.

**Keywords** Early warning signal · Abrupt climate change · Kurtosis coefficient · Critical point

## 1 Introduction

Critical phenomena exists in many types of complex systems, which means that the system has critical thresholds, i.e. critical points, in which the system is very likely to shift abruptly from one relatively stable state to another new state (Alley et al. 2003; Ding et al. 2006, 2007; Li and Chou 1996, 1997; Lin and North 1997; May 1977; Scheffer et al. 2009; Sun and Mu 2009). This transition is often large, abrupt, and widespread change (Ding et al. 2009, 2010, 2016; Evtushovsky et al. 2018; Rietkert 2004; Scheffer et al. 2001; Warren et al. 2004; Xiao et al. 2007; Sun and Mu 2011).

In physics, the system's behavior or structure will change drastically around the critical point. For example, the phase transition from solid to liquid or from liquid to gaseous is a typical critical phenomenon. Another interesting example is the phenomenon of phase change in magnetic systems. When the temperature of a magnetic system is greater than a certain critical threshold, the magnetization of the magnetic system is 0. However, when the temperature is less than the critical threshold, the magnetization of the system is related to its temperature, geometric dimension, and the dimension of the order parameter (Ising 1925). In a sandpile model, when the slope of the sandpile reaches a certain critical threshold, dropping another grain of sand onto the sandpile may cause nothing, or it may cause the entire sandpile to collapse in a massive slide (Bak et al. 1987). In the three typical critical phenomena mentioned above, the control parameters of the first two phenomena are temperature and the third one is the slope of the sandpile. The common feature of these critical phenomena is that the state of the system will experience a substantial shift if the certain control parameter of the system is forced across the critical threshold.

Technically, an abrupt climate change occurs when the climate system is forced to cross some threshold, triggering

✉ Wen-ping He  
wenping\_he@163.com

<sup>1</sup> Department of Physics, Institute of Space Weather, Nanjing University of Information Science and Technology, Nanjing 210044, China

<sup>2</sup> National Climate Center, China Meteorological Administration, Beijing 100081, China

<sup>3</sup> Collaborative Innovation Center on Forecast and Evaluation of Meteorological Disasters, Nanjing University of Information Sciences and Technology, Nanjing 210044, China

a transition to a new state (National Research Council reports 2002). Abrupt climate change can occur on various different time scales which have been verified by a number of climatic records (Alley et al. 2003; Hansen et al. 2015; Gómará et al. 2016; Lenton et al. 2008; Li et al. 1996; Moreno-Chamarro et al. 2017; Wang et al. 2018; Xiao et al. 2012). A well-known example for abrupt climate change is the Younger Dryas event, which persists about from 12.9 ka BP to 11.7 ka BP (Firestone et al. 2007). In this event, a gradual climatic warming after the Last Glacial Maximum was temporarily reversed to glacial conditions, which lasted for nearly a thousand years. In recent years, global atmosphere–ocean system occurred a decadal abrupt change in 1970s (Hare et al. 2000; Jacques-Coper 2015; Miller et al. 1994; Warren et al. 2004; Xiao et al. 2007). The physical climate system, natural systems, and human systems could also be severely affected by abrupt climate changes which have occurred repeatedly throughout the geological record. Therefore, it is urgent to carry out research on the mechanisms, prediction techniques, and theories of abrupt climate change. In particular, it is very important to study the early warning signal for abrupt climate change, which will help people and government take actions to adapt any impending abrupt climate change with large and unanticipated impacts in future.

Unfortunately, because of the complexity and nonlinearity of the climate system, it is difficult in the climate system to conduct those experiments similar to that in physics and chemistry (Feng et al. 2003, 2004; Li et al. 1996, 1997). At present, some mechanisms of past abrupt climate changes have been revealed. However, many mechanisms are still merely inference based on various assumptions. From the point of view of the simulation capabilities of the existing climate models (He et al. 2018; Kumar et al. 2013; Zhao and He 2015), even if the proposed mechanism seems reasonable, it is still difficult to simulate the past abrupt climate changes with high accuracy. Although the performances of various climate models have been improving, they still cannot be used to quickly achieve accurate predictions of abrupt climate change. Therefore, based on the current capabilities of climate prediction, it is undoubtedly an extremely difficult task to predict such critical transitions in the climate system.

Encouragingly, some generic properties have been revealed before several different types of dynamical system near their own critical thresholds (Carpenter and Brock 2006; Dakos et al. 2012; Guttal and Jayaprakash 2008; van Nes and Scheffer 2007; Wissel 1984). These generic properties have no relation to the detailed description of each system, that is, regardless of the specific mathematic form of each dynamical system (Scheffer et al. 2009). For example, three distinctly different phenomena, including extinction of population caused by excessive hunting, catastrophic regime shifts in ecosystems (Rietkert et al. 2004), and paleoclimatic

transitions can be expressed using the same information, i.e., a significant increase in autocorrelation was found before reaching the critical point which can be regarded as precursors of transitions.

Several early warning indicators for abrupt change have been presented, including increased variance, increased autocorrelation, slower recovery from perturbations, changing skewness, increased long-range correlation and flickering when a dynamical system approaches a critical point (Carpenter and Brock 2006; Dakos et al. 2012; Guttal and Jayaprakash 2008; van Nes and Scheffer 2007). Some comparative studies of the performance of early warning signals have been conducted, and the results indicated that there was no single universal method for warning an impending abrupt change (Dakos et al. 2012). Therefore, it is crucial to evaluate the performance of an early warning indicator of an abrupt change.

The climate system exhibits a complex and nonlinear characteristic, which cannot be accurately simulated by climate models at present (Feng et al. 2009; Fraedrich and Blender 2003). Simple fold models could provide useful information into the ways to approach a critical point beyond which an abrupt change will occur (Guttal et al. 2008). A system will exhibit asymmetry when the system approaches some critical thresholds (Guttal et al. 2008). Based on this, the kurtosis coefficient is used as an early warning signal for an abrupt change (Biggs et al. 2009). However, they don't systematically investigate the performance of the kurtosis coefficient as an early warning indicator, as well as the influence of noise and missing data. In present paper, we systematically investigate the performance of the kurtosis coefficient as an early warning signal for upcoming abrupt climate change. Similar to the reference (Guttal et al. 2008), two routes to abrupt change have been investigated in this paper: an abrupt change occurs as a control parameter approaches a critical point or as increasing the magnitude of stochastic external forcing.

In the present paper, we first introduce briefly the definition of the kurtosis coefficient, and some simple fold models which are used to generate the model time series for abrupt change. In Sect. 3, the performance of the kurtosis coefficient is systematically investigated, as well as the influence of the missing data and observational noise. Section 4 presents the conclusion and a briefly discussion.

## 2 Method and models

### 2.1 Definition of kurtosis coefficient

In practice, it can often be found that the data with the same variance have different sharpness of the probability distribution. In probability theory and statistics, the kurtosis is

usually used to quantitatively describe the sharpness of a probability distribution, namely, measure the “tailedness” of the probability distribution. The fourth-order central moment divided by the standard deviation of the fourth power is defined as the kurtosis coefficient which has been presented as follows:

$$k = \frac{\frac{1}{N} \sum_{i=1}^N (x_i - \mu)^4}{\sigma^4}. \tag{1}$$

The parameters  $\mu$  and  $\sigma$  are the mean and standard deviation of a time series  $\{x_i, i = 1, \dots, N\}$ , respectively. The kurtosis coefficient is 3 for a univariate normal distribution. The kurtosis coefficient less than 3 means a platykurtic distribution compared with the normal distribution. If the kurtosis coefficient is greater than 3, the distribution is leptokurtic. Generally speaking, an adjusted version of kurtosis coefficient is often used in practice, i.e., the excess kurtosis, which is defined by the kurtosis coefficient  $- 3$ . In this paper, we use the excess kurtosis as the kurtosis coefficient if there is no special instruction.

## 2.2 Fold models

In this paper, three simple fold models have been used to generate model time series for investigating the performance of the kurtosis coefficient as an early warning when these models approach a critical threshold. In this section, we briefly introduced the three models used in present paper.

### 2.2.1 Univariate population growth model

The logistic equation has been widely applied in various fields, such as abrupt climate change, chaos, ecological contexts (May 1976, 1977; He et al. 2013). In present paper, a generalized logistic model is used to simulate vegetation density in semi-arid regions. The model is mainly developed on the basis of the continuous logistic equation, which describes the nonlinear relationship between the vegetation biomass and the growth rate of grazing rate as well as the carrying capacity of ecosystem. And the generalized population growth model has been shown as follows (Noy-Meir 1975; May 1977; Guttal and Jayaprakash 2008).

$$\frac{dV}{dt} = rV \left( 1 - \frac{V}{K} \right) - c \frac{V^2}{V^2 + V_0^2} + \sigma_V \eta_V(t). \tag{T1}$$

According to the reference (Guttal and Jayaprakash 2008), the constant  $r$  represents the intrinsic growth rate of vegetation biomass and the parameter  $K$  characterizes the carrying capacity of ecosystem. In this study, the values of the constant  $r$  and the parameter  $K$  are 1 and 10, respectively.

The variable  $V$  is the vegetation biomass. The control parameter  $c$  is the maximum grazing rate which ranges from 1 to 3.  $V_0$  is the characteristic vegetation biomass at which the growth rate is half the maximum, which is taken as  $V_0 = 1$ .  $\sigma_V$  represents the standard deviation of external noise which ranges from 0 to 1. The stochastic variable  $\eta_V$  is uncorrelated Gaussian noise, which satisfies the following relationship:

$$\langle \eta_V(t) \eta_V(t') \rangle = \delta(t - t').$$

### 2.2.2 Time-delayed population growth model

On the basis of Eq. (T1), a time-delayed model has been presented (T1.1). There is a lag term and a multiplicative noise  $\sigma_r \eta_r(t)$  that simulates the fluctuation in the grazing rate in the model (Guttal et al. 2013).

$$\frac{dV(t)}{dt} = rV(t) \left( 1 - \frac{V(t - \tau)}{K} \right) - [c + \sigma_c \eta_c(t)] \frac{V(t)^2}{V(t)^2 + V_0^2}. \tag{T1.1}$$

### 2.2.3 Bivariate coupled model of soil–water and vegetation

This model can be used to simulate the abrupt change of the vegetation in semi-arid regions caused by overgrazing. Different from the univariate population growth model (Eq. T1), the nonlinear interaction between soil–water and vegetation has been taken account into this model (Guttal and Jayaprakash 2007, 2008).

$$\begin{aligned} \frac{dw}{dt} &= R - \alpha w - \lambda w B + \sigma_w \eta_w(t) \\ \frac{dB}{dt} &= \rho B \left( w - \frac{B}{B_c} \right) - \mu \frac{B}{B + B_0} + \sigma_B \eta_B(t). \end{aligned} \tag{T2}$$

Here, rainfall (evaporation) will increase (decrease) the soil water  $w$ . In this model, the rainfall rate is represented by the parameter  $R$  which ranges from 0 to 3, and the  $-\alpha w$  term represents the evaporation (In this study,  $\alpha = 1.0$ ). The negative feedback term  $-\lambda w B$  is the uptaking rate of water by vegetation with  $\lambda = 0.12$  in our test. The values of the parameters  $\rho$  and  $B_c$  are 1 and 10, respectively. The other two parameters are  $B_0 = 1$  and  $\mu = 2$ ,  $\sigma_w$  and  $\sigma_B$  represent the standard deviation of the fluctuations in the rainfall rate and the external noise, which both range from 0 to 1. The stochastic variable  $\eta_w$  and  $\eta_B$  are uncorrelated Gaussian noise.

### 2.2.4 Trivariate model

The third model is a relatively complex parameterized ecological model of lake eutrophication (slightly modified version of Carpenter and Brock 2006; Guttal and Jayaprakash 2008).

$$\begin{aligned}
 \frac{dP}{dt} &= l - (s + h)P + [r + \sigma_r \eta_r(t)]MR(P) + \sigma_l \eta_l(t) \\
 \frac{dM}{dt} &= sP - bM - [r + \sigma_r \eta_r(t)]MR(P) \\
 R(P) &= \frac{P^q}{P_0^q + P^q}.
 \end{aligned}
 \tag{T3}$$

The variables  $P$  and  $M$  are the phosphorus concentration in water and sediment, respectively. The parameter  $l$  ranges from 0.5 to 1.0, which reflects the loading rate of the nutrient to a lake. The outflow rate  $h$  and the recycling coefficient  $r$  are 0.15 and 0.019, respectively. The parameter  $b$  is 0.001 and  $P_0 = 2.4$  is the Hill coefficient. The stochastic variable  $\eta_l(t)$  is an additive noise term and  $\eta_r(t)$  is a multiplicative noise, and they reflect the fluctuation influence of stochastic events on the variables  $P$  and  $M$ , respectively. The detailed physical meaning of the model can be found in the reference (Guttal and Jayaprakash 2008).

All of the stochastic differential equations used in this study are solved numerically by a simple Euler algorithm (Guttal and Jayaprakash 2008). Unless otherwise stated, the length of each model time series used to calculate the kurtosis coefficient is 2000 time unites with a time step  $dt=0.1$ , namely, the sample size is 20,000, and the results for early warning test are the average of the kurtosis coefficient over 100 such experiments in each model.

### 3 Results

With the increase of the maximum grazing rate  $c$  in the model (T1), univariate population growth model exhibits an abrupt change of vegetation biomass when the parameter  $c$  is greater than the critical threshold, which is presented in Fig. 1. In this study, the two bifurcation points in the model (T1) are  $c^* = 1.8$  and  $c^* = 2.6$ , respectively. The univariate model shows a single stable state with relatively higher vegetate density for  $c < 1.8$  than that for  $c > 2.6$ . However, a bistable with two stable equilibrium states will occur for  $1.8 < c < 2.6$ , namely, coexisting high-density and low-density vegetated states. In mathematics, stability theory addresses the stability of solutions of differential equations and of trajectories of dynamical systems under small perturbations of initial conditions. Stability means that the trajectories do not change too much under small perturbations. A stable equilibrium state can be identified by the method provided by the website ([https://en.wikipedia.org/wiki/Stability\\_theory](https://en.wikipedia.org/wiki/Stability_theory)).

In order to intuitively display the change of kurtosis of time series generated by a dynamical system when the system closes to a critical threshold, the two time series and corresponding histograms are presented in Fig. 2 when the

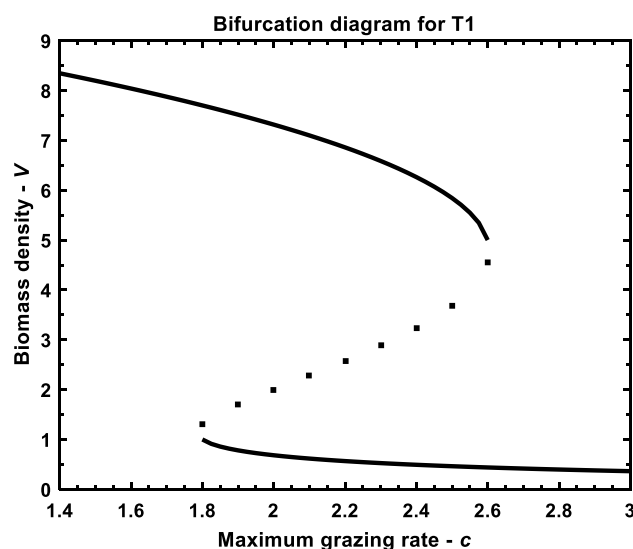


**Fig. 1** The bifurcation diagram for the univariate population growth model (Eq. T1) in which the continuous increase in grazing rate  $c$  can result in an abrupt change of the biomass density  $V$ . The thick solid lines correspond to stable ecological states, and the dotted line indicates the unstable equilibrium states

parameter  $c$  in the Eq. (T1) takes the values of 1.5 and 2.1, respectively. Obviously, the parameter  $c = 2.1$  is closer to the critical threshold ( $c^* = 2.6$ ) than  $c = 1.5$ , and the distribution for  $c = 2.1$  is more flat than that for  $c = 1.5$ . In other words, there is an obvious change in kurtosis of the time series of the state variable  $V$  of Eq. (T1) with the increase of the parameter  $c$  (Fig. 2), i.e., the values of the kurtosis coefficient are 0.028325 for  $c = 1.5$  and 0.8792 for  $c = 2.1$ , respectively. Therefore, the change of parameters will lead to a significant change in the probability density distribution of the system's state variable. The origin of the asymmetry and the rise in kurtosis as the transition is approached can be found in the reference (Guttal et al. 2008).

In the first route, the parameter  $c$  in Eq. T1 is gradually increased forward to the critical threshold  $c^* = 2.6$ , and we fix the magnitude of the external noise  $\sigma_V$  (i.e., the standard deviation of the noise). The results indicate that the kurtosis coefficient exhibits a small fluctuation which is very close to zero about for  $c < 1.7$ . As the parameter  $c$  continues to increase, an obvious increase of the kurtosis coefficient can be found (Fig. 3a). This increased trend is even more pronounced for about  $c > 2.15$ . Therefore, the kurtosis will be substantially changed as the parameter  $c$  approaches the critical threshold ( $c^* = 2.6$ ) in Eq. T1. Moreover, we also test the performance of the kurtosis coefficient when the parameter  $c$  approaches another critical threshold of the Model T1 in this study, i.e.,  $c^* = 1.8$ . The results similar to Fig. 3a can be obtained (Fig. 3b).

The existing results indicate that even if the parameter in a system is far from its critical point, the increase

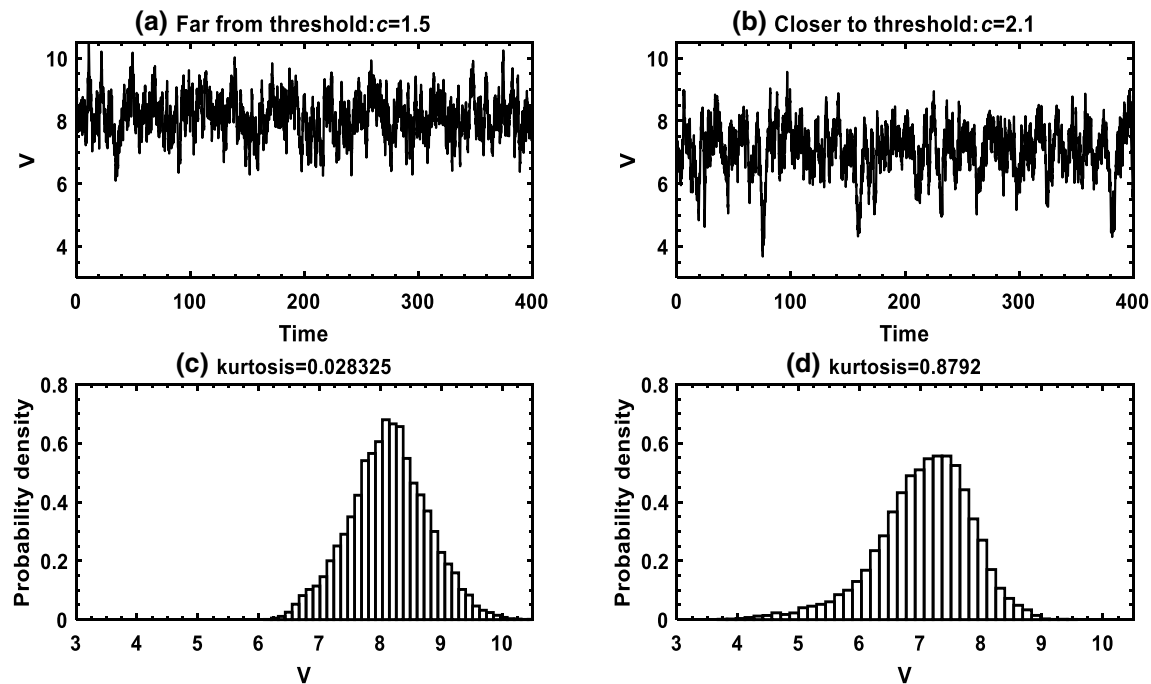


**Fig. 2** The time series for two representative numerical results which were generated by the univariate population growth model, and corresponding probability density: **a** the model time series for the parameter  $c=1.5$  in which the system is far from the critical threshold ( $c^*=2.6$ ); **b** the model time series for the parameter  $c=2.1$  in which the system is closer to the critical threshold ( $c^*=2.6$ ) than that for  $c=1.5$ ; **c** the probability density of the time series shown in **a**; **d** the

probability density of the time series shown in **b**. The kurtosis of the biomass density is also calculated for each realization. The initial conditions are the high biomass density as shown in the bifurcation diagram. Here, we choose  $\sigma_V = 0.75$ , a time step of  $dt = 0.01$  and 400 time units for time series. Rest of the parameters is same as in Sect. 2.2

of stochastic external forcing can also result in an abrupt change (Guttal and Jayaprakash 2008). According to the second way to abrupt change, we fix the parameter  $c$  in Eq. T1 with the value of 2.0, and gradually increase the strength of the external noise  $\sigma_V$ . Obviously, the parameter  $c=2.0$  is far from the critical threshold of the system ( $c^*=2.6$ ) (Fig. 1). The results indicate that there is negligible influence on the change of kurtosis for a relatively weak external forcing, i.e., for about  $\sigma_V < 0.23$  (Fig. 3c). With the further increase of the strength of the stochastic external forcing  $\sigma_V$ , the kurtosis coefficient gradually becomes larger and larger (Fig. 3c). A similar result can be obtained when the parameter  $c$  is taken other values and kept a constant, and the strength of the stochastic external forcing  $\sigma_V$  is gradually increased (Figures omitted).

In practice, there are different degrees of observation error in all types of observational data, such as the error caused by observation instruments. Thus, it is very crucial to investigate the influence of the observation error on the performance of the kurtosis coefficient as an early warning signal for an upcoming abrupt change. Based on this, three kinds of strong noises (represents observation error) have been studied in the present paper. All of model time series generated by Eq. T1 can be regarded as the observational

data, and then uncorrelated Gaussian noise is superimposed to these model time series. The strengths of the noise with different signal to noise ratios (SNR) are 5 dB, 10 dB, and 20 dB, respectively. The corresponding analyzed results are shown in Fig. 4. In the tests for the first route to abrupt change, the relatively weak observation error (i.e., SNR=20 dB) has a negligible influence on the change of kurtosis. However, with the increase of the magnitude of the observation error, an obvious effect can be found, such as SNR=10 dB and 5 dB (Fig. 4a). In other words, strong noise greatly shortens the effective warning time for early warning signal of kurtosis. Moreover, strong noise also causes the amplitude of kurtosis to be largely diminished during the system approaches the critical threshold. It is worth to be pointed that although the noise (i.e., observation error) has a great influence on the changing magnitude and warning time of kurtosis coefficient, especially for relatively strong noise, the kurtosis coefficient still provides an effective early warning. For example, the SNR=5 dB means a strong noise in a signal, and the standard deviation of the signal with SNR=5 dB is much greater than that of the original model time series. Thus, the kurtosis coefficient as an early warning signal has an anti-noise ability to some extent when the parameter  $c$  is slowly increased along the upper branch of the bifurcation



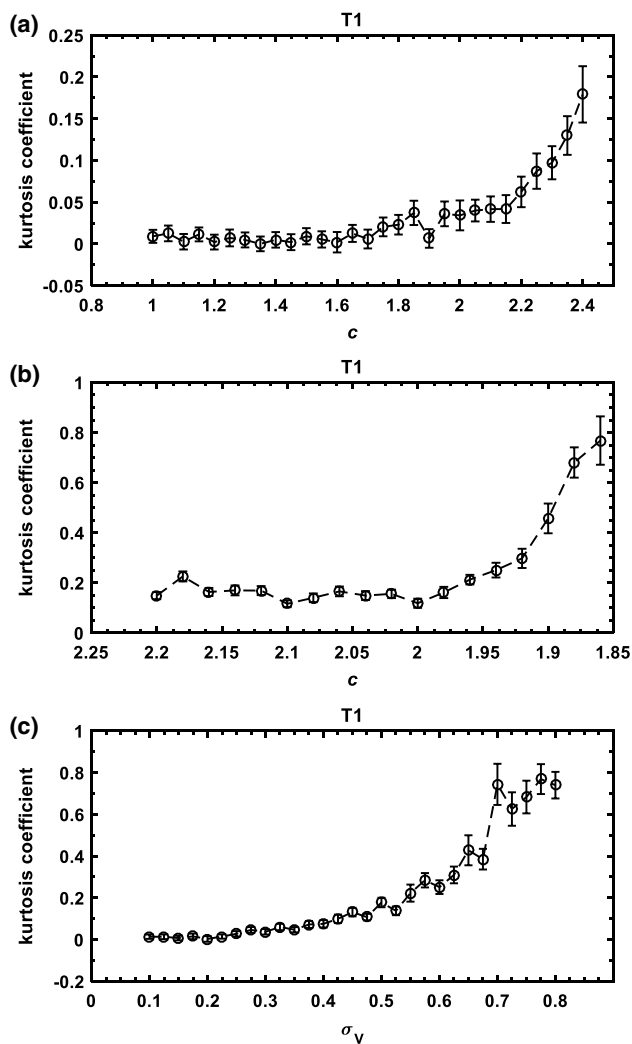


**Fig. 3** The kurtosis coefficient increases as a function of the parameter  $c$  and the standard deviation of external noise  $\sigma_V$  when the ecosystem approaches the threshold via different routes for the Model T1. The open circles represent the average kurtosis coefficient calculated by the numerical simulations, and the error-bar shows the standard deviation of mean for such 100 experiments. The dashed line aims at guiding the eye. **a** Increasing the parameter  $c$  to approach the critical threshold  $c^* = 2.6$ , and keeping the external fluctuations unchanged, i.e.,  $\sigma_V = 0.25$ ; **b** same as **a** but for decreasing the parameter  $c$  to approach another critical threshold  $c^* = 1.8$ ; **c** Increasing  $\sigma_V$  with the fixed parameter  $c = 2.0$

diagram of Model T1. However, strong noise results in that the kurtosis coefficient does not work when decreasing the parameter  $c$  to approach another critical threshold  $c^* = 1.8$  (Fig. 4c). Therefore, it is important to consider the effect of strong noise on the effective of the kurtosis coefficient as an early warning signal in practice.

In the second route to abrupt change, the influence of noise with relatively weak intensity on the warning results of kurtosis coefficient can almost be ignored, i.e., for SNR = 20 dB. After increasing the intensity of the observational error,

namely, the standard deviation of the error, the influence of noise gradually comes out, namely, the greater the intensity of noise is, the greater the influence is. The strong noise results in the shortened warning time to a certain degree, and the amplitude of the kurtosis coefficient is also reduced. However, there is still enough time to warn an upcoming abrupt change using changing kurtosis under strong observational error (Fig. 4e). Even for the situation of the strong noise (SNR = 5 dB), the kurtosis coefficient gradually increases from about  $\sigma_V = 0.4$ , in which the system is far from its critical threshold of the external forcing (greater than 0.8).

Missing data is an inevitable phenomenon which often occurs in practice. Thus, it is important to investigate the influence of missing data on the performance of an early warning indicator. On the basis of this, we present the results of the kurtosis coefficient for various time series with different extents of missing data in this study. In our numerical simulation, missing data is simulated by randomly removing some data from the model time series used in Fig. 3, and then we calculate the kurtosis coefficients of the new time series which are removed some data with a certain length for each experiment. Finally, the average kurtosis coefficient for such 100 experiments can be obtained. We exhibit the results for four kinds of losing rate of data, including 5% loss, 10% loss, 15% loss, and 20% loss, respectively. Surprisingly, the missing data has almost no significant effect on the early warning ability of the kurtosis coefficient whether for increasing the parameter  $c$  or increasing the strength of external noise (Fig. 4b, d, f).

In order to further test the effectiveness of the kurtosis coefficient as a warning signal, the kurtosis coefficient is applied in a more complex nonlinear interaction model (Eqs. T2) than Eq. T1. The bivariate coupled model of soil–water and vegetation exhibits a fold bifurcation between the vegetable biomass  $B$  and the rainfall rate  $R$ , and the bifurcation diagram is shown in Fig. 5a. The two bifurcation points are  $R^* \approx 1.06$ , and  $R^* \approx 2.0$ , respectively. A bistable will occur for  $1.06 < c < 2.0$ , in which the vegetated state to the bare state will coexist. In the first route to an abrupt change, the strength of external forcing  $\sigma_B = 0.25$  is fixed. With the decrease of the parameter  $R$ , the ecosystem will occur an abrupt change from the vegetated state to the bare state. It can be found that the kurtosis coefficient is very close to the zero when the parameter  $R$  is far from the critical threshold  $R^* \approx 1.06$  (Fig. 5b). After the parameter  $R$  is reduced to the value of 1.4, the kurtosis coefficient exhibits a slow increase. With the parameter  $R$  is further reduced to about 1.25, the kurtosis coefficient shows a trend of rapid increase. Obviously, the changing kurtosis can be regarded as an effective early warning signal when the parameter of the system (T2) approaches the critical threshold  $R^* \approx 1.06$ .

We also tested the performance of the kurtosis coefficient in the second route to an abrupt change by using the

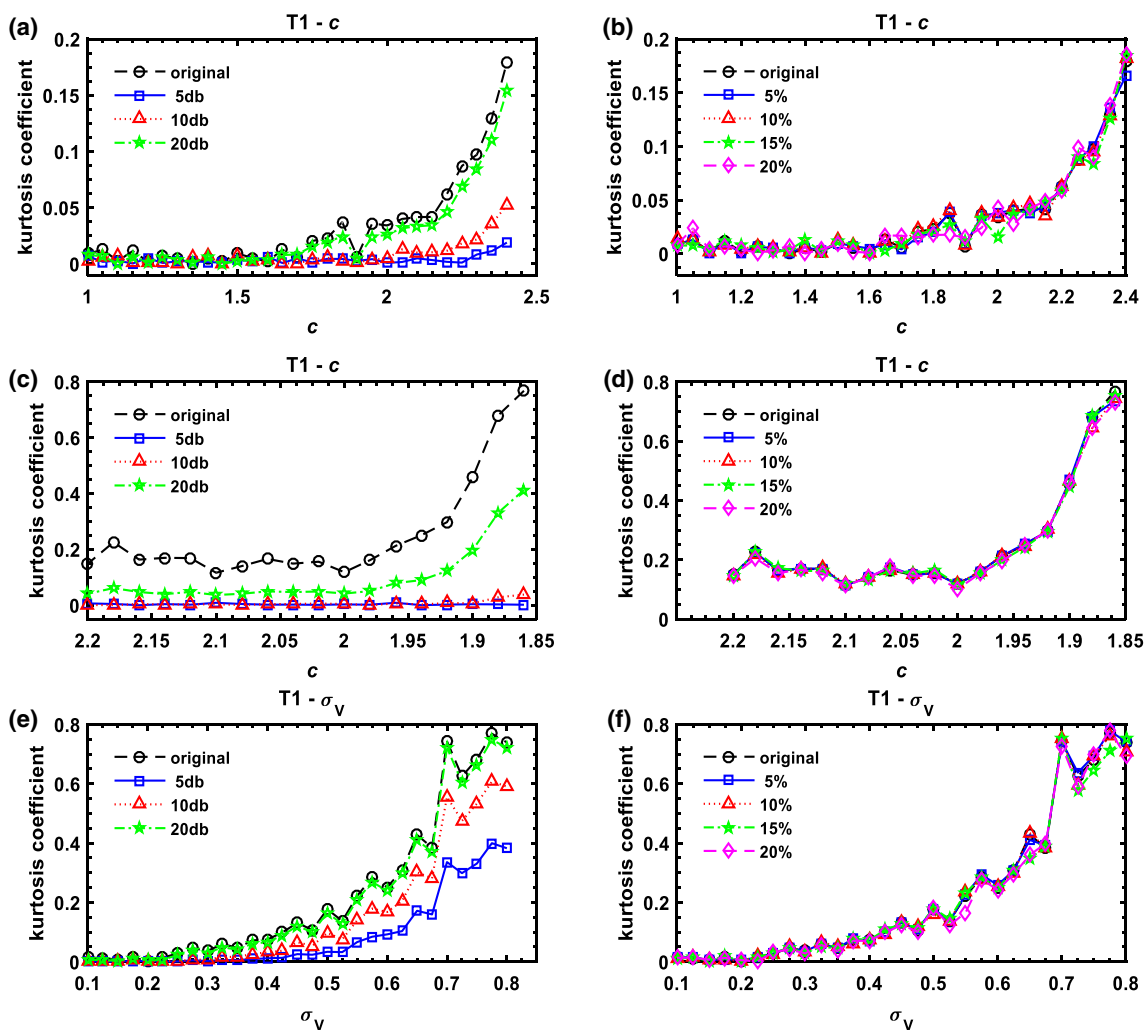


**Fig. 4** Influence of the observational error on the effective of the kurtosis coefficient **a** and **c** for the first route, and **e** for the second route. Influence of the missing data on the effective of the kurtosis coefficient **b** and **d** for the first route, and **f** for the second route

bivariate coupled model of soil–water and vegetation (T2). In this test, the parameter of rainfall rate is fixed by  $R = 1.5$ , which is far from the critical threshold  $R^* \approx 1.06$ , and the standard deviation of the fluctuations in the rainfall rate is kept a constant, i.e.,  $\sigma_w = 0.01$ . Then, we gradually increase the strength of the external noise  $\sigma_B$ , and find that there is no significant trend in kurtosis coefficient for  $\sigma_B < 0.3$  (Fig. 5c). With the increase of the strength of the external noise, the kurtosis coefficient exhibits a significant increasing trend for  $\sigma_B > 0.3$  (Fig. 5c). We select two representative cases which are far from and close to the corresponding critical threshold (Fig. 6). It is very easy to be found by the naked eye that the system exhibits a distinctly different distribution pattern when it is far from the threshold and close to the threshold. Thus, the kurtosis coefficient works well whether for the first route to an abrupt change or for the second one. The results verify that it is effective to present an early warning signal

based on the changing kurtosis coefficient in the bivariate coupled model.

Based on the model time series used in the Fig. 5, the effects of the observational errors and the missing data on the performance of the kurtosis coefficient as an early warning signal are investigated. The results indicate that the kurtosis coefficient has an anti-noise ability to some extent (Fig. 7a, c). In spite of this, the strong noise can greatly shorten the effective warning time of the kurtosis coefficient. Moreover, the strong noise can also result in the greatly reduction of the magnitude of the kurtosis coefficient. That is, the stronger the noise, the shorter the warning time, and the smaller the changing magnitude in the warning signal. The influence of the missing data on the kurtosis coefficient is shown in the Fig. 7b, d, it could be concluded that the missing data has almost negligible effect on the kurtosis coefficient. No significant effect can be found even when the

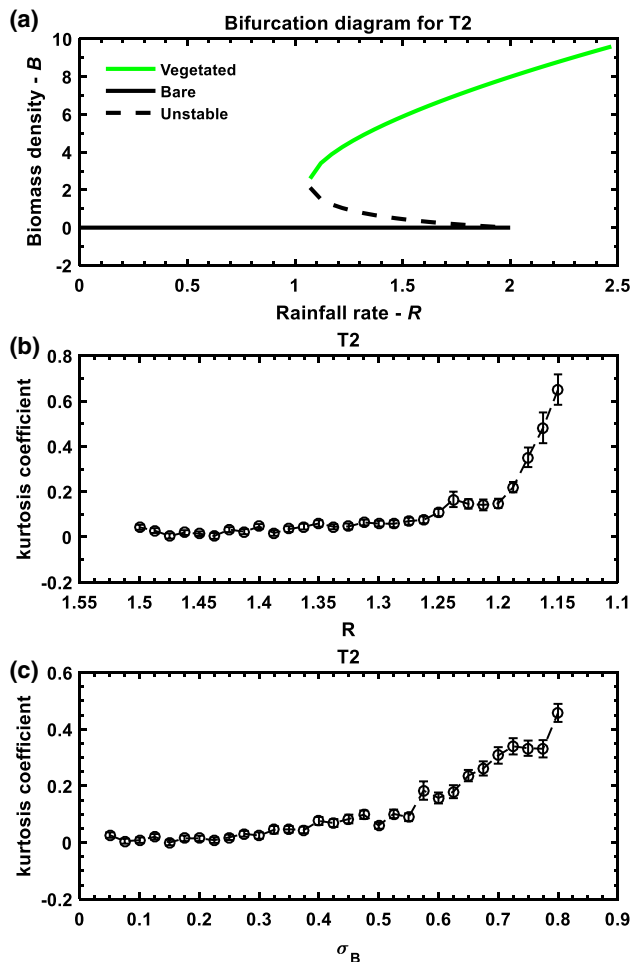


**Fig. 5** The results for the two variable vegetation model (T2). **a** The bifurcation diagram with two bifurcation points correspond to  $R^* \approx 1.06$  and  $R^* \approx 2.0$ ; **b** approaching the bifurcation point ( $R^* \approx 1.06$ ) by reduction in rainfall rate,  $R$ , fixing the external fluctuations  $\sigma_B = 0.25$  and the fluctuations of soil water  $\sigma_w = 0.01$ ; **c** the kurtosis coefficient as a function of the external fluctuation  $\sigma_B$  with the fixed rainfall rate  $R = 1.5$  (far from the threshold) and  $\sigma_w = 0.01$ . The error-bar shows the standard deviation of mean

missing data accounted for 20% of the total sample whether for the first route or for the second route (Fig. 7b, d).

Similar to the parameter settings in the bivariate vegetation model used in Fig. 5, we only change the standard deviation of the fluctuations in the rainfall rate  $\sigma_w$  from 0.01 to 0.25 in the model T2. In other words,  $\sigma_w = 0.25$  and  $\sigma_B = 0.25$  (the strength of external forcing) are kept constant in the first route to abrupt change for the bivariate vegetation model. The results indicate that with the decrease of the parameter  $R$ , a significant trend of increase can be found when the system is far from the critical threshold  $R \approx 1.06$  (Fig. 8a). In the second route to abrupt change for the bivariate vegetation model, we keep the rainfall rate  $R$  and the standard deviation of the fluctuations in the rainfall rate  $\sigma_w$  unchanged, i.e.,  $R = 1.5$  (far from the threshold) and

$\sigma_w = 0.25$  (obviously greater than 0.01 used in Fig. 5c), and then gradually increase the strength of the external fluctuation  $\sigma_B$ . A rapidly increasing trend can be found by naked eyes when the strength of external fluctuation  $\sigma_B$  is greater than about 0.22 (Fig. 8b).

When we only increase the standard deviation of the fluctuations in the rainfall rate  $\sigma_w$ , and fix the rainfall rate ( $R = 1.5$ ) and the strength of external forcing ( $\sigma_B = 0.25$ ), the kurtosis coefficient has no significant changes (Fig. 8c), which is completely different from the first two cases in Fig. 8 for only increase  $R$  or  $\sigma_B$ . The result indicates that the kurtosis coefficient does not work for an upcoming abrupt change in the third case (Fig. 8c).

The third model (T3) is also used to test the performance of the kurtosis coefficient as an early warning signal when a dynamical system approaches its critical threshold. The model is a more complex ecological model than the first two models, which describes the dynamics of a lake eutrophication. The bifurcation diagrams of the model T3 are presented in Fig. 9a, b. In our numerical simulations, the length of time series is taken as  $T = 70$ ,  $dt = 0.01$ . The initial values are taken as  $P(t = 0) = 1$ , and  $M(t = 0) = 800$ , respectively. The last 60 time units are used to calculate the kurtosis coefficient in order to ensure the system in equilibrium from the initial state. The results indicate that there is relatively small fluctuation of the kurtosis coefficient as a function of the parameter  $l$  for  $l < 0.9$ . A significant increasing trend can be found for  $l > 0.9$  (Fig. 9c).

Figure 10 provides two model time series, in which the parameter  $l$  is far from or close to the critical threshold ( $l^* \approx 0.975$ ). It can be easy to find that the probability distribution of the phosphorus concentration  $P$  in water is wider for  $l = 0.83$  than that for  $l = 0.5$ , namely, the tails of the distribution for  $l = 0.83$  asymptotically approach zero more slowly than that for  $l = 0.5$ . The results indicate that the changing kurtosis coefficient can capture an early warning signal when the parameter  $l$  of the model (T3) approaches its critical threshold.

Different from the first two models, the observational error has relatively larger influence on the results of the kurtosis coefficient, i.e., the kurtosis coefficient does not work under three noise cases (Fig. 11a). Similar to the results of the first two models, the missing data has almost negligible effect on the kurtosis coefficient, even when the missing data accounted for 20% of the total sample size (Fig. 11b).

From a view of nonlinear interaction and long-range correlation of a dynamical system, nonlinear feedbacks which are not always instantaneous can be captured by time-delayed models to some extent. For example, the impact of volcanic eruptions on global climate will continue for many years, namely, the forcing effects are not instantaneous instead of a time lag. Thus, it is more practical to study the applicability of an early warning indicator for an abrupt



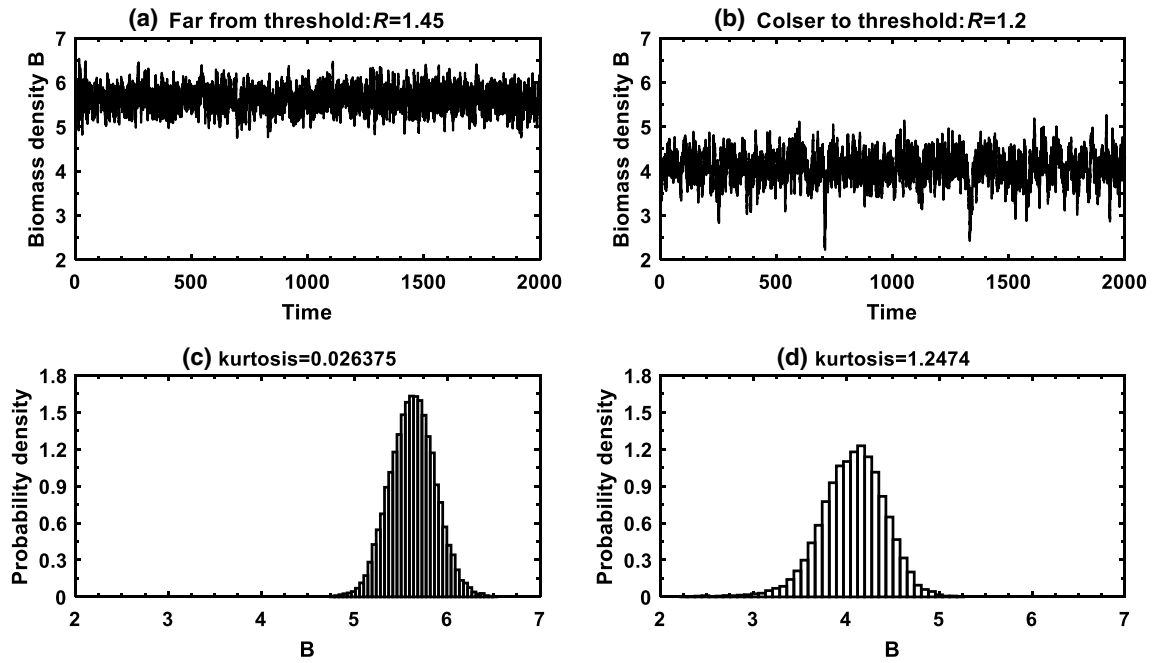


Fig. 6 Same as Fig. 2 but for the two variable vegetation model (T2)

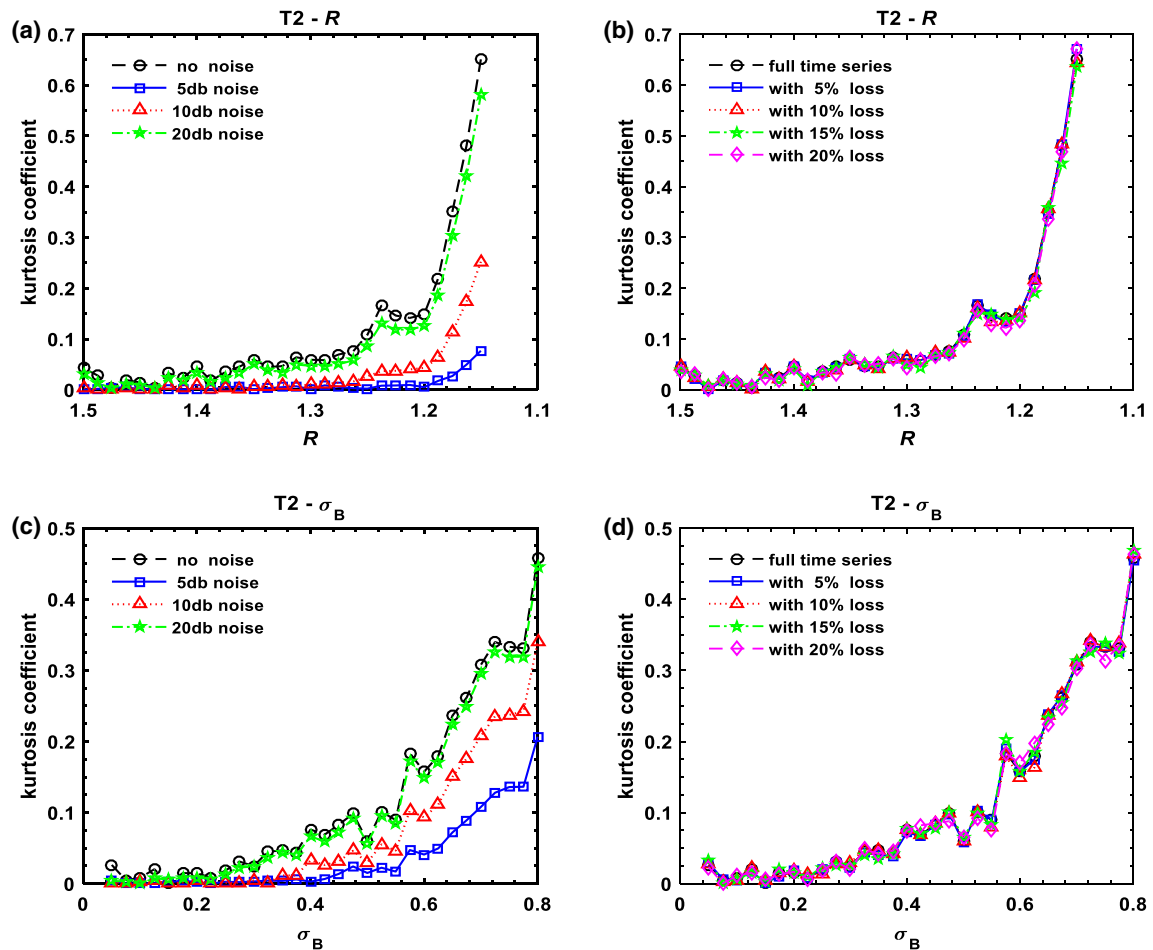
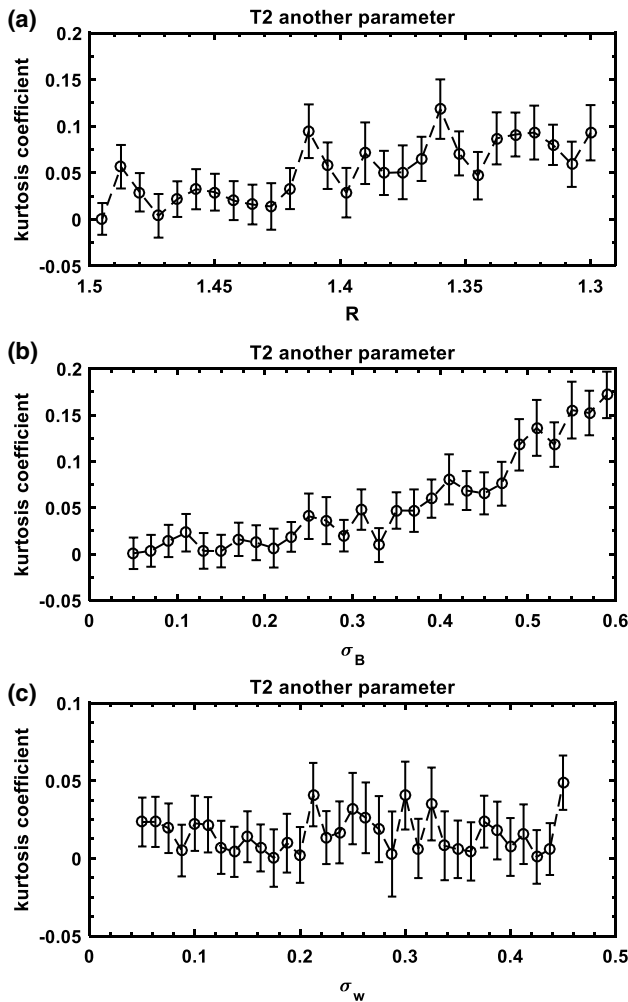


Fig. 7 Same as Fig. 4, but for the two variable vegetation model (T2)



**Fig. 8** The results for the bivariate vegetation model (T2). **a, b**: kurtosis increases when system is approaching threshold via two paths, the parameters in model T2 are same as those used in Fig. 5 but for  $\sigma_w = 0.25$ ; **c** increasing  $\sigma_w$ , and keeping  $R = 1.5$ ,  $\sigma_B = 0.25$  unchanged. The error-bar shows the standard deviation of mean

change occurs in a time-delay model than that in instantaneous one.

In the time-delayed population growth model, the bifurcation points are the same as Fig. 1. The initial value is not a single value but an array of values because of the time delay term. We choose a relatively high biomass density  $V = 5$  as the value of each element in the array, and the length of the array depends on the time delay term. The length of time series  $T = 1050$ ,  $dt = 0.1$ . The first 50 time unites during the integration process are discarded as a transient in which the system will enter into equilibrium vial the initial state. So, the last 1000 time unites will be used to calculate the kurtosis coefficient. We then average the kurtosis coefficient over 200 such experiments. Figure 12 shows the results for the time delay  $\tau = 1.7$ , which indicate that the kurtosis coefficient

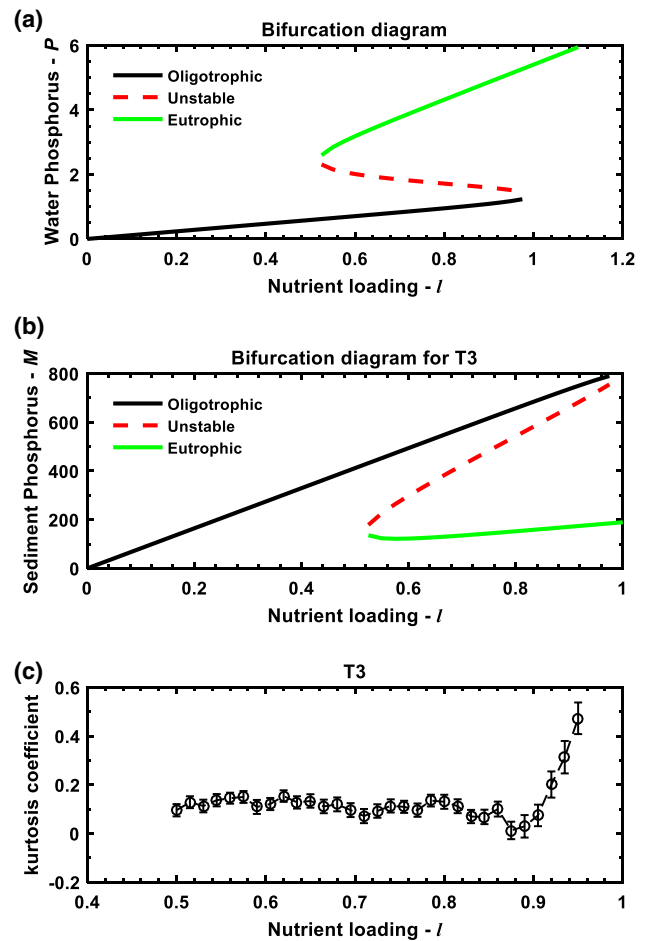


**Fig. 9** The results for the parameterized lake eutrophication model (T3). **a, b** The bifurcation diagram as a function of nutrient loading  $l$ . The black thick lines show the stable oligotrophic states and the green thick lines express the stable eutrophic state, whereas the red dotted lines represent the unstable equilibria. The two thresholds of the collapse are  $l^* \approx 0.5$  and  $l^* \approx 0.975$ , respectively; **c** the average kurtosis coefficient of lake eutrophic model as a function of the nutrient loading  $l$ . The error-bar shows the standard deviation of mean

significantly decreases as the increase of the grazing rate  $c$ . The decreasing trend can be found even when the system is far away from the critical threshold, for example, the parameter  $c$  varies from 1.0 to 1.3 which is obviously far away from the threshold  $c^* = 2.6$ . Moreover, the changing kurtosis coefficient can be intuitively found from its probability density map when the system is close to the critical threshold, such as the probability density for  $c = 1.0$  and  $c = 2.1$  (Fig. 13).

The existence of the observational noise can result in different influences which depend on the strength of the observational noise (Fig. 14a). In spite of this, the kurtosis coefficient still can give an effective early warning for an abrupt change. Even it is still true for strong noise. The results further prove that the kurtosis coefficient has an anti-noise

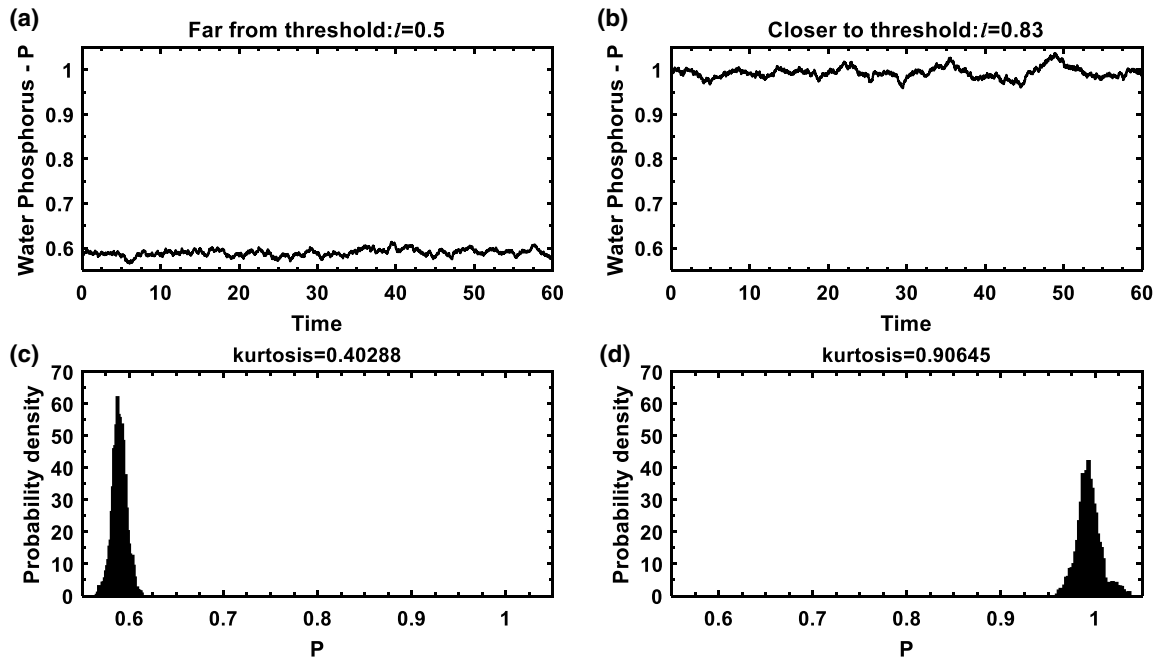


Fig. 10 Same as Fig. 2 but for the model (T3)

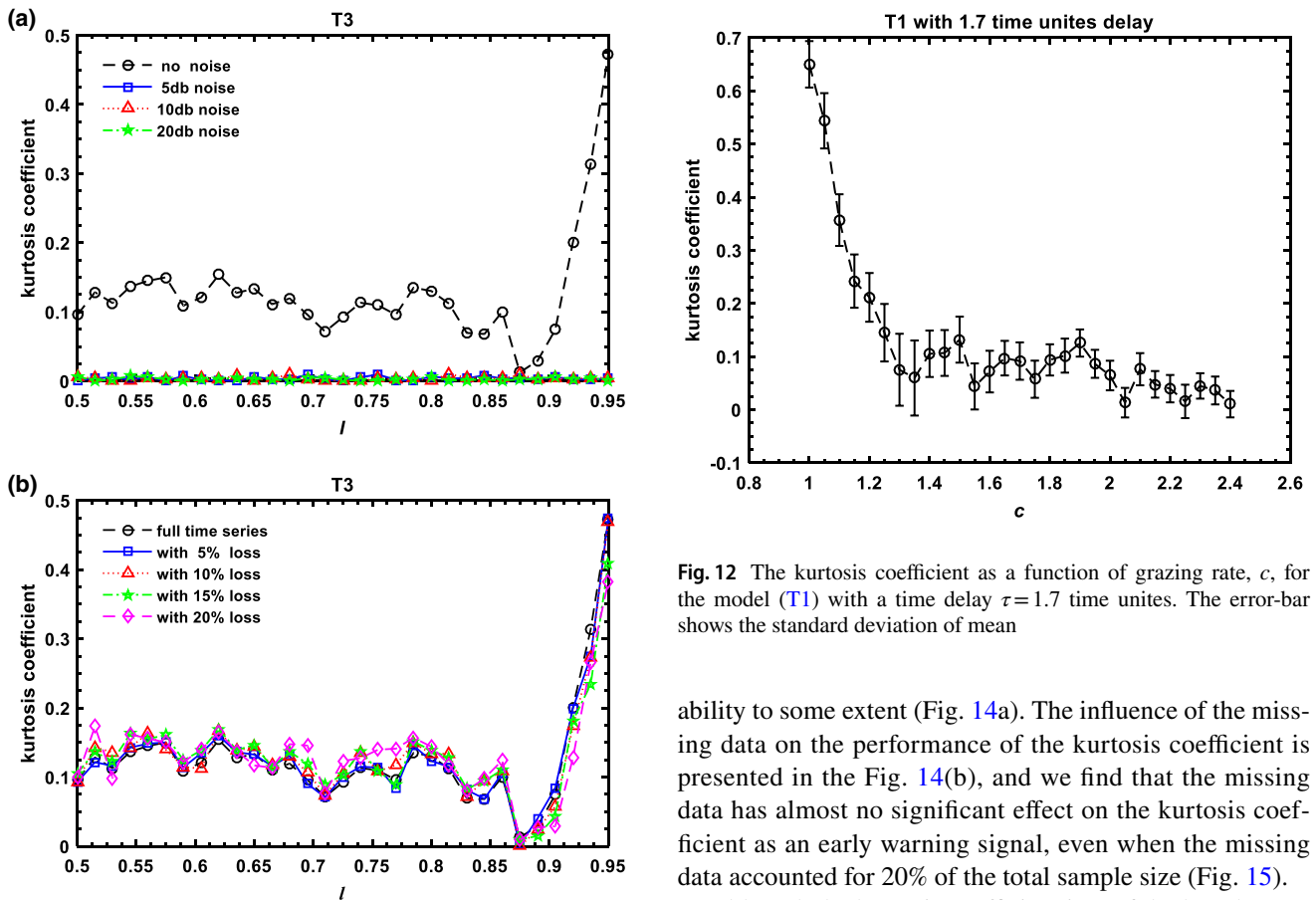


Fig. 11 The effects of the observational error and missing data on the kurtosis coefficient tested by Lake model (T3)

Fig. 12 The kurtosis coefficient as a function of grazing rate,  $c$ , for the model (T1) with a time delay  $\tau = 1.7$  time unites. The error-bar shows the standard deviation of mean

ability to some extent (Fig. 14a). The influence of the missing data on the performance of the kurtosis coefficient is presented in the Fig. 14(b), and we find that the missing data has almost no significant effect on the kurtosis coefficient as an early warning signal, even when the missing data accounted for 20% of the total sample size (Fig. 15).

Although the kurtosis coefficient is useful when the system approaches its threshold for the time delay of  $\tau = 1.7$ , the kurtosis coefficient cannot exhibit an obvious change

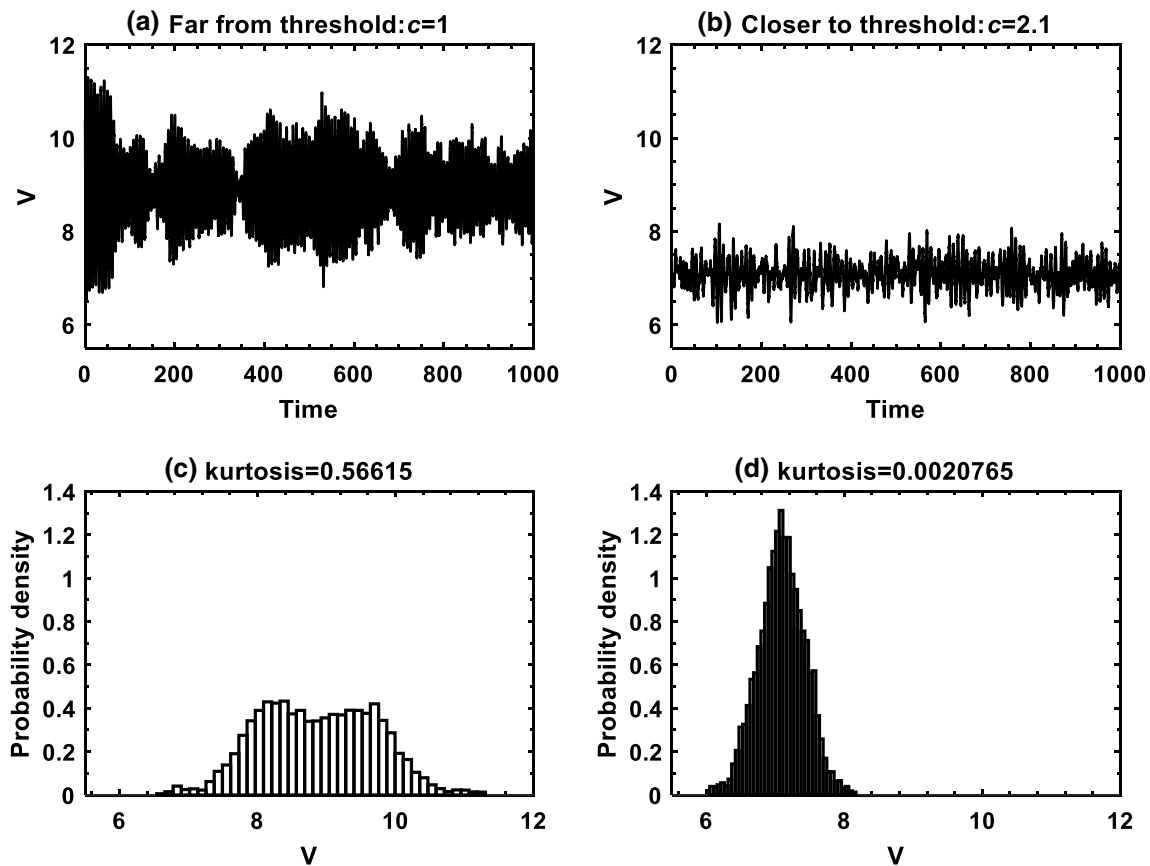


Fig. 13 Same as Fig. 2 but for the model (T1) with a time delay  $\tau = 1.7$  time units

when the grazing rate  $c$  closes to the critical threshold ( $c^* = 2.6$ ) for the model (T1) with a time delay of  $\tau = 1.0$ . The result indicates that the kurtosis coefficient does not work for the time-delayed feedback processes  $\tau = 1.0$ . So, two completely different results are obtained when the delay times are  $\tau = 1.7$  and  $\tau = 1.0$  in the model (T1), respectively, which means that the kurtosis coefficient is not universal warning indicator for an upcoming abrupt change.

#### 4 Discussion and conclusions

Many dynamical systems have the critical thresholds, including the climate system, ecosystem, economic system, etc. When a system goes beyond its critical threshold, an abrupt change of the system's state will occur. Obviously, it is very difficult to predict such critical transitions in the climate system as well as other dynamical systems. In recent years, a lot of studies indicate that an early warning signal of abrupt climate change or regime shift in ecosystems is traceable. In this paper, we test the performance of the kurtosis coefficient as an early warning signal for an

impending abrupt change by using different simple nonlinear models, including univariate population growth model, bivariate coupled model of soil–water and vegetation, a relatively complex parameterized ecological model of lake eutrophication, as well as time-delayed population growth model. Our results show that the kurtosis coefficient is a good indicator for an upcoming abrupt change in most of cases in our tests.

The strong noise can greatly shorten the effective warning time of the kurtosis coefficient, and also can result in the reduction of the changing magnitude of the kurtosis coefficient when a dynamical system is close to the critical threshold, even the kurtosis coefficient does not work in some cases. The missing data has almost no significant effect on the kurtosis coefficient as an early warning signal in all of tests. The conclusion is still true even when the missing data accounted for 20% of the total sample size in this study.

Moreover, we also found that the kurtosis coefficient did not show significant changes when a dynamical system is close to its critical threshold including delay model and non-delay model. In other words, the kurtosis coefficient does not work in these two cases. The results mean that the

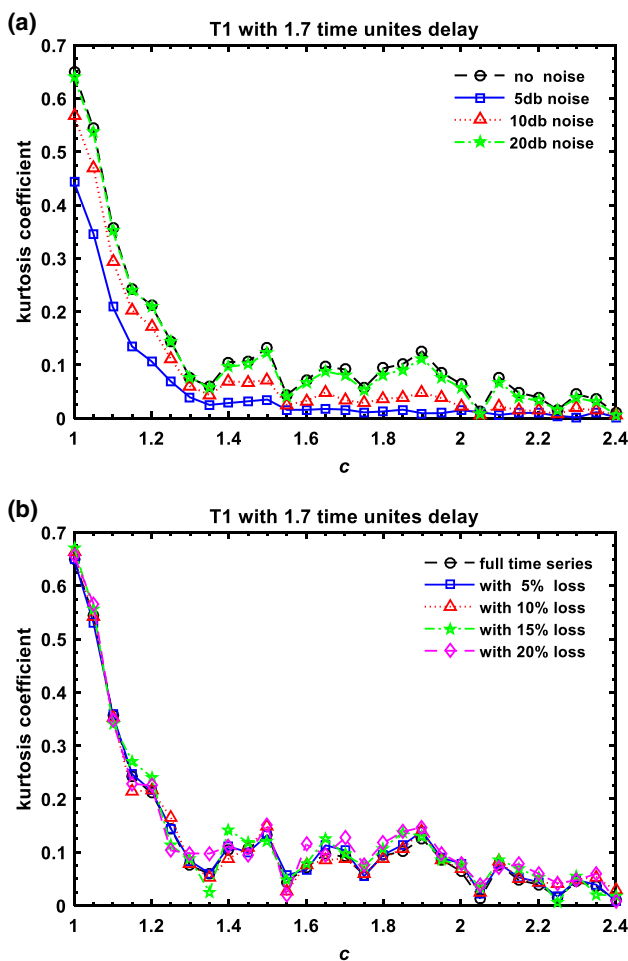


**Fig. 14** The effects of noise (a) and the missing data (b) on the kurtosis coefficient tested in the model (T1) with 1.7 time unites delay

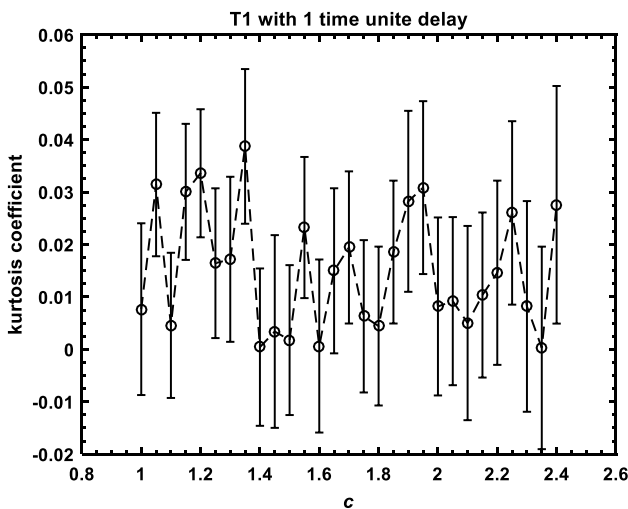


**Fig. 15** The kurtosis coefficient for the model (T1) with a time delay of  $\tau = 1.0$ . We obtained the kurtosis via the same way as the time delay of 1.7. In this case, kurtosis does not work. The error-bar shows the standard deviation of mean

kurtosis coefficient has a certain scope of application, and no single early warning indicator can solve all of cases of abrupt change. So, it is very crucial to develop multiple early warning signals for a relatively reliable warning.

**Acknowledgements** The authors would like to thank the three anonymous reviewers and editors for the beneficial and helpful suggestions for this manuscript. This research was jointly supported by National Natural Science Foundation of China (Grant nos. 41775092, 41605069, 41475073, 41530531, and 41475064).

## References

Alley RB, Marotzke J, Nordhaus WD, Overpeck JT, Peteet DM, Pielke RA, Pierrehumbert RT, Rhines PB, Stocker TF, Talley LD, Wallace JM (2003) Abrupt climate change. *Science* 299:2005–2010. <https://doi.org/10.1126/science.1081056>

Bak P, Tang C, Wiesenfeld K (1987) Self-organized criticality: an explanation of  $1/f$  noise. *Phys Rev Lett* 59(4):381–384

Biggs R, Carpenter SR, Brock WA (2009) Turning back from the brink: Detecting an impending regime shift in time to avert it. *Proc Nat Acad Sci USA* 106:826–831

Brock W (2006) Tipping points, abrupt opinion changes and punctuated policy change. In: Repetto RP (ed) *Punctuated equilibrium and the dynamics of US environmental policy*. Yale University Press, New Haven, pp 47–77

Carpenter SR, Brock WA (2006) Rising variance: a leading indicator of ecological transition. *Ecol Lett* 9:308–315

Committee on Abrupt Climate Change, National Research Council (2002) “Definition of abrupt climate change”. *Abrupt climate change: inevitable surprises*. National Academy Press, Washington, DC. ISBN 978-0-309-07434-6

Dakos V, Carpenter SR, Brock WA, Ellison AM, Guttal V et al (2012) Methods for detecting early warnings of critical transitions in time series illustrated using simulated ecological data. *PLoS One* 7(7):e41010

Ding RQ, Li JP (2009) Decadal and seasonal dependence of North Pacific SST persistence. *J Geophys Res* 114:D01105. <https://doi.org/10.1029/2008JD010723>

Ding RQ, Feng GL, Liu SD, Liu SK, Huang SX, Fu ZT (2006) Review of the study of nonlinear atmospheric dynamics in China (2003–2006). *Adv Atmos Sci* 24:1077–1085

Ding Y, Ren G, Zhao Z, Xu Y, Luo Y, Li Q, Zhang J (2007) Detection, causes and projection of climate change over China: an overview of recent progress. *Adv Atmos Sci* 24:954–971

Ding RQ, Ha KJ, Li JP (2010) Interdecadal shift in the relationship between the East Asian summer monsoon and the tropical Indian Ocean. *Climate Dyn* 34:1059–1071

Ding RQ, Li J, Tseng YH, Ha KJ, Zhao S, Lee JY (2016) Interdecadal change in the lagged relationship between the Pacific–South American pattern and ENSO. *Clim Dyn Online*. <https://doi.org/10.1007/s00382-016-3002-1>

Evtushevsky OM, Grytsai AV, Milinevsky GP (2018) Decadal changes in the central tropical Pacific teleconnection to the Southern Hemisphere extratropics. *Clim Dyn*. <https://doi.org/10.1007/s00382-018-4354-5>

Feng GL, Dong WJ (2003) Evaluation of the applicability of a retrospective scheme based on comparison with several difference schemes. *Chin Phys* 12:1076–1086

Feng GL, Dong WJ (2004) Application of retrospective time integration scheme to the prediction of torrential rain. *Chin Phys* 13:413–422



- Feng GL, Wang QG, Hou W, Gong ZQ, Zhi R (2009) Long-range correlation of extreme events in meteorological field. *Acta Phys Sin* 58:2853–2861
- Firestone RB, West A, Kennett JP et al (2007) Evidence for an extra-terrestrial impact 12,900 years ago that contributed to the megafaunal extinctions and the Younger Dryas cooling. *Proc Natl Acad Sci USA* 104(41):16016–16021
- Fraedrich K, Blender R (2003) Scaling of atmosphere and ocean temperature correlations in observations and climate models. *Phys Rev Lett* 90:108501–108501
- Gómara I, Rodríguez-Fonseca B, Zurita-Gotor P et al (2016) Abrupt transitions in the NAO control of explosive North Atlantic cyclone development. *Clim Dyn* 47:3091. <https://doi.org/10.1007/s00382-016-3015-9>
- Guttal V, Jayaprakash C (2007) Impact of noise on bistable ecological systems. *Ecol Model* 201:420–428
- Guttal V, Jayaprakash C (2008) Changing skewness: an early warning signal of regime shifts in ecosystems. *Ecol Lett* 11(5):450–460
- Guttal V, Jayaprakash C, Tabbaa OP (2013) Robustness of early warning signals of regime shifts in time-delayed ecological models. *Theor Ecol* 6:271–283
- Hansen J, Sato M, Hearty P et al (2015) Ice melt, sea level rise and superstorms: evidence from paleoclimate data, climate modeling, and modern observations that 2 °C global warming is highly dangerous. *Atmos Chem Phys Discuss* 15:20059–20179
- Hare SR, Mantua NJ (2000) Empirical evidence for North Pacific regime shifts in 1977 and 1989. *Prog Oceanogr* 47:103–145
- He WP, Wan SQ, Jiang YD, Jin HM, Zhang W, Wu Q, He T (2013) Detecting abrupt change on the basis of skewness: numerical tests and applications. *Int J Climatol* 33(12):2713–2727. <https://doi.org/10.1002/joc.3624>
- He WP, Zhao SS, Wu Q, Jiang YD, Wan SQ (2018) Simulating evaluation and projection of the climate zones over China by CMIP5 models. *Clim Dyn*. <https://doi.org/10.1007/s00382-018-4410-1>
- Ising E (1925) Beitrag zur theorie des ferromagnetismus. *Z Phys* 31:253–258
- Jacques-Coper M, Garreaud RD (2015) Characterization of the 1970s climate shift in South America. *Int J Climatol* 35:2164–2179. <https://doi.org/10.1002/joc.4120>
- Kumar S, Merwade V, Kinter JL, Niyogi D (2013) Evaluation of temperature and precipitation trends and long-term persistence in CMIP5 Twentieth-century climate simulations. *J Clim* 26(12):4168–4185
- Lenton TM, Held H, Kriegler E, Hall JW, Lucht W, Rahmstorf S, Schellnhuber HJ (2008) Tipping elements in the Earth's climate system. *Proc Natl Acad Sci* 105(6):1786–1793
- Li JP, Chou JF (1996) The property of solutions for the equations of large-scale atmosphere with the non-stationary external forcings. *Chin Sci Bull* 41(7):587–590
- Li JP, Chou JF (1997) The effects of external forcing, dissipation and nonlinearity on the solutions of atmospheric equations. *Acta Meteor Sin* 11(1):57–65
- Li JP, Chou JF, Shi JE (1996) Detecting methods on the mean value jump of the climate. *J Beijing Meteorol Coll* 2:16–21. (In Chinese)
- Lin RQ, North GR (1990) A study of abrupt climate change in a simple nonlinear climate model. *Clim Dyn* 4:253. <https://doi.org/10.1007/BF00211062>
- May RM (1976) Simple mathematical models with very complicated dynamics. *Nature* 261(5560):459–467
- May RM (1977) Thresholds and breakpoints in ecosystems with a multiplicity of stable states. *Nature* 269:471–477
- Miller AJ, Cayan DR, Barnett TP, Oberhuber JM (1994) The 1976–77 climate shift of the Pacific Ocean. *Oceanography* 7:996–1002
- Moreno-Chamarro E, Zanchettin D, Lohmann K, Jungclaus JH (2017) An abrupt weakening of the subpolar gyre as trigger of little ice age-type episodes. *Clim Dyn* 48:727. <https://doi.org/10.1007/s00382-016-3106-7>
- Noy-Meir I (1975) Stability of grazing systems: an application of predator-prey graphs. *J Ecol* 63:459–482
- Rietkert M, Dekker SC, Ruiter PC, Koppel J van de (2004) Self-organized patchiness and catastrophic shifts in ecosystems. *Science* 305:1926–1929
- Scheffer M, Carpenter SR, Foley JA, Folke C, Walker B (2001) Catastrophic shifts in ecosystems. *Nature* 413:591–596
- Scheffer M, Bascompte J, Brock WA, Brovkin V, Carpenter SR, Daskov V, Held H et al (2009) Early-warning signals for critical transitions. *Nature* 461(7260):53–59
- Sun GD, Mu M (2009) Nonlinear feature of the abrupt transitions between multiple equilibria states of an ecosystem model. *Adv Atmos Sci* 26(2):293–304
- Sun GD, Mu M (2011) Response of a grassland ecosystem to climate change in a theoretical model. *Adv Atmos Sci* 28(6):1266–1278
- van Nes EH, Scheffer M (2007) Slow recovery from perturbations as a genetic indicator of a nearby catastrophic shift. *Am Nat* 169:738–747
- Wang C, Wang B, Wu LG (2018) Abrupt breakdown of the predictability of early season typhoon frequency at the beginning of the twenty-first century. *Clim Dyn*. <https://doi.org/10.1007/s00382-018-4350-9>
- Warren SW, Chang IZ (2004) Regime shifts in the North Pacific: early indications of the 1976–1977 event. *Prog Oceanogr* 60:183–200
- Wissel C (1984) A universal law of the characteristic return time near thresholds. *Oecologia* 65:101–107
- Xiao D, Li J (2007) Spatial and temporal characteristics of the. *J Geophys Res*. <https://doi.org/10.1029/2007JD008956>
- Xiao D, Li J, Zhao P (2012) Four-dimensional structures and physical process of the decadal abrupt changes of the northern extratropical ocean-atmosphere system in 1980s. *Inter J Climatol* 32:983–994
- Zhao SS, He WP (2015) Evaluation of the performance of the Beijing Climate Centre Climate System Model 1.1(m) to simulate precipitation across China based on long-range correlation characteristics. *J Geophys Res*. <https://doi.org/10.1002/2015JD024059>

**Publisher's Note** Springer Nature remains neutral with regard to jurisdictional claims in published maps and institutional affiliations.